PHYSICAL REVIEW D VOLUME 22, NUMBER 7 1 OCTOBER 1980

Clustering and hadronization of quarks: A treatment of the low-p_T problem

Rudolph C. Hwa
Institute of Theoretical Science and Department of Physics, University of Oregon, Eugene, Oregon 97403
(Received 20 November 1979; revised manuscript received 6 February 1980)

The low-p_T problem of hadron fragmentation is treated in the framework of the quark model. The basic mechanism of hadronization of quarks is recombination, which is formulated here on a firm basis. Clustering of quarks in a hadron is discussed in detail. The quark and antiquark joint distribution is derived systematically with incorporation of quantum-chromodynamics ideas wherever possible. Parameters describing the distribution are determined by fitting low-Q^2 electroproduction data. No free parameters are therefore involved in the calculation of the pion inclusive distribution in the fragmentation region. The result agrees well with data in both shape and normalization. The formalism can be applied to calculate inclusive distributions of all nucleon- and pion-initiated reactions, while for kaon-initiated reactions it can be used to extract from low-p_T data the quark distributions in kaons.

I. AN OVERVIEW OF THE PROBLEM

Strong interactions in the realm of hard processes, such as large-p_T reactions and massive-lepton-pair production, have in recent years come within grasps of quantitative theoretical investigations in the framework of quantum chromodynamics (QCD). However, soft processes such as low-p_T reactions do not yet enjoy a similar status, since the long-distance behavior at low momentum transfer is closely enmeshed with the confinement problem which is still unsolved. Nevertheless, despite the lack of a reliable calculational procedure, significant progress has been made during the past two years in discovering and understanding the connection between inclusive cross sections in the fragmentation region and the momentum distributions of quarks in hadrons. In this paper we build upon that connection a formulation of the low-p_T problem at the constituent level. Clearly, we do not yet have a theory for rigorous calculations from first principles. But we shall insofar as possible incorporate into the formulation ideas derivable from QCD and find dynamical description of quantities that were introduced with some arbitrariness in earlier models.

The quark model for inclusive reactions in the fragmentation region that we refer to above is the recombination model.[1] It was Ochs[2] who first pointed out the similarity between the inclusive pion distribution for pp reactions and the structure function of the proton in deep-inelastic scattering, although the question of how the quarks turn into hadrons was left open. Das and Hwa[3] showed that the fragmentation model for hadronization is phenomenologically unacceptable, and suggested a specific recombination mechanism that can give good fits to the data. The preoccupation at that time was to demonstrate that the idea of recombination is phenomenlogically sensible both in normalization as well as in x dependence. To that end a simple formula was proposed[3]:

$$\frac{x}{\sigma}\frac{d\sigma}{dx} = \int F(x_1,x_2)R(x_1,x_2,x)\frac{dx_1}{x_1}\frac{dx_2}{x_2}, \tag{1.1}$$

where $F(x_1,x_2)$ is the two-parton joint distribution for the incident hadron and $R(x_1,x_2,x)$ is the recombination function. On the basis of the counting rule[4] it was suggested that $R(x_1,x_2,x)$ for a meson should have the form

$$R(x_1,x_2,x) = \alpha\frac{x_1x_2}{x}\delta(x_1+x_2-x), \tag{1.2}$$

where α is an unknown normalization constant of order unity. The two-parton distribution is more difficult to determine precisely. As a simple first trial the naive factorizable form was suggested:

$$F(x_1,x_2) = F_q(x_1)F_{\bar{q}}(x_2)\rho(x_1,x_2), \tag{1.3}$$

where F_q and $F_{\bar{q}}$ are the distributions of a quark q and an antiquark $\bar{q}$, and $\rho(x_1,x_2)$ is a phase-space factor proportional to $1-x_1-x_2$ for proton, but later extended to a more general form.[5] With these ingredients satisfactory agreement with data was achieved,[3] giving support to the importance of the recombination mechanism. Later, Duke and Taylor[6] succeeded in obtaining detailed fits of various inclusive distributions, using (1.1)–(1.3).

A major effort in the subsequent development of the recombination model has focused on various improved forms of $F(x_1,x_2)$ and their implications. In place of (1.3) a Kuti-Weisskopf model[7] for $F(x_1,x_2)$ has been suggested.[8-10] While it succeeds in satisfying certain kinematical constraints, it remains a phase-space model with uncertain dynamical content. The difficulty is, of course, the unsolved bound-state problem of the hadrons. A way to circumvent that difficulty while still examining the recombination model is to study photon-

initiated reactions[11] or quark jets.[12] Within certain approximations the function $F(x_1,x_2)$ for photon and quark (or gluon) can be calculated in perturbative QCD. Our problem at hand is to formulate a way of calculating $F(x_1,x_2)$ for hadrons by tackling the bound-state problem on the one hand and incorporating ideas from the QCD calculations on the other.

In the absence of an adequate understanding of the confinement problem, the wave function of the constituent quarks in a hadron must to a large extent be phenomenological. Since that wave function must influence the structure function measured at high Q^2, it should be possible to extract that information from recent data. In Ref. 13 we have adopted the view that the partons in a nucleon form three clusters, called valons. The momentum distribution of the valons is determined from the Q^2 dependence of the structure functions. This will be discussed in Sec. II for both nucleons and mesons. The valon distribution will turn out to play a crucial role in determining not only $F(x_1,x_2)$, but also the recombination function $R(x_1,x_2,x)$. Although we cannot at this stage derive it from first principles, its concept is dynamically sound and its quantitative features are reliably determined from phenomenology based on QCD.

Going from the valon distribution to the quark and antiquark joint distribution involves gluon bremsstrahlung and quark-pair production. The cummulative effect of such conversion processes is hard to determine at low Q^2. In order to arrive at a reasonable formulation of this problem, it is useful to recall the parton-model description of multiparticle production. Feynman invented the parton model specifically for low-p_T reactions.[14] Scaling of inclusive cross sections was predicted as a consequence of scale-invariant parton distributions, which in turn were suggested by the structure functions determined at SLAC. Although the Q^2 value was as low as 1 GeV^2, the scaling phenomenon was already sufficiently evident to be called "precocious." In the context of QCD where scaling violation is understood as Q^2 evolution due to gluon bremsstrahlung,[15] precocious scaling is then equivalent to mature evolution. Indeed, if even at $Q^2 \simeq 1$ GeV^2 the gluons carry nearly half the nucleon momentum, and the wee parton distribution is already scaling, gluon bremsstrahlung must be so highly effective for $Q^2 < 1$ GeV^2 that by $Q^2 \gtrsim 1$ GeV^2 (what is usually called low Q^2) the major part of the evolution has already taken place. It is important to recognize this in order to start from Feynman's ideas about low-p_T reactions and develop a more quantitative calculational scheme such as we shall pursue in Sec. V.

Our aim will be to address the major issues in formulating the low-p_T problem, without being involved in the detailed fits of various reactions. Our concern will be the general scheme rather than specific processes. Thus, for example, we shall not emphasize the flavor dependence of quark types or mesons produced, but the question of how both the normalization and shape of $\sigma^{-1} x\, d\sigma/dx$ are to be determined will be examined carefully. The formulation lends itself in a straightforward way to more elaborate treatments that account for all types of beam and detected particles.

It should be pointed out that the approach taken here is very different from the ones adopted by the groups at Lund, Orsay, and Saclay.[16] They emphasize quark fragmentation and borrow phenomenological description of the fragmentation functions from hard-scattering processes without addressing the basic problem of hadronization, i.e., how the quarks turn into hadrons.

Another approach to the low-p_T problem is by means of the counting rules by Brodsky and Gunion[17] and more recently by Gunion,[18] considering "pointlike" diagrams. They start from the $x \to 1$ limit and examine simple Feynman diagrams in QCD that are regarded as dominant in the large-x region.

In our approach we emphasize the main part of the x region, excluding the extreme limits of $x \to 0$ and $x \to 1$. There are a few parameters in our formulation, but they are completely fixed by the structure functions of the nucleon. Obviously, we need some phenomenological input on the quark distribution, for example. However, after those parameters are determined, the formalism fully specifies the low-p_T problem. There are no free parameters to adjust. Inclusive cross sections of all reactions can be calculated. Our result for pion production from proton agrees well with data in both shape and normalization.

The organization of the paper is as follows. We first discuss the valons and their momentum distributions in Sec. II, followed by the determination of the recombination function in Sec. III. We then outline the problem of calculating the quark decay function (Sec. IV), which will serve as a guide to the main problem of hadron fragmentation discussed at length in Sec. V. The conclusion is given in the final section.

II. VALON DISTRIBUTIONS IN HADRONS

Valence-quark clusters, called valons,[13] form a natural bridge between constituent quarks in the bound-state problem of the hadrons and the partons as probed in deep-inelastic scattering.[19] A valon is defined to be a dressed valence quark in QCD. That is, it is a valence quark together with its cloud of gluons and sea quarks which can be resolved by high-Q^2 probes. At sufficiently low Q^2

the internal structure of a valon can no longer be resolved, but at the hadron mass scale it should be possible to distinguish individual valons in a hadron. A nucleon has three valons and a meson has two valons, just like the constituent quarks. The momentum distributions of the valons are independent of the Q^2 values of the probe. The structure of a valon itself is, however, Q^2 dependent. Assuming that a quark is basically pointlike, at least for the distance scale that can be probed in the foreseeable future, the structure functions of a valon are then completely determined by gluon bremsstrahlung and quark-pair creation in the framework of QCD. Indeed, they are just the "structure functions" of a quark.[20]

For hadron fragmentation the valon distribution in a hadron is of primary importance. It describes the uncalculable wave function of the constituent quarks. Before discussing how it is to be used in a low-p_T reaction, we describe first how it is determined. On the basis of the definition we have given above, and assuming that in a deep-inelastic scattering the probing of the structure of one valon is not influenced by the interaction of that valon with other spectator valons (the usual impulse approximation), we can write

$$\mathcal{F}^h(x,Q^2)=\sum_v \int_x^1 dy\, G_{v/h}(y)\mathcal{F}^v(x/y,Q^2)\,, \qquad (2.1)$$

where $\mathcal{F}^h$ is the structure function of hadron h (e.g., F_2, xF_3, etc.), $\mathcal{F}^v$ is the corresponding structure function of valon v, and $G_{v/h}$ is the distribution of v in h. The symbol x is the momentum fraction of probed quark in hadron h, while y is the momentum fraction of a valon in the same hadron. The sum is over various flavor types of v. A pictorial representation of (2.1) for one of the valons being probed is shown in Fig. 1. The right-hand side of (2.1) has an implicit dependence on a variable Q_v that specified the value of Q at which the valons are resolved as individual units acting as constituent quarks, but with no discernible internal structure. We postpone our discussion on this point until later.

As we have indicated in Sec. I, we shall not in this paper be concerned with flavor dependence of $G_{v/h}$. To distinguish flavor differences would require more accurate data than we now have for phenomenological analysis. The theoretical problem of accounting for the differences is easy, and a more complete analysis shall be carried out when the muon scattering data at high Q^2 become available. Thus, for now we consider only an average valon distribution, whose normalization is

$$\int_0^1 G_{v/h}(y)dy = 1 \qquad (2.2)$$

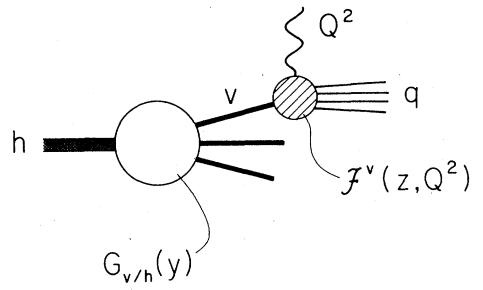

FIG. 1. A schematic diagram showing that the structure function of a hadron h is a convolution of the valon distribution in h and the structure function of the valon.

and which satisfies the momentum sum rule

$$\int_0^1 G_{v/h}(y)y\,dy = \tfrac{1}{3} \quad (h=\text{nucleon}) \qquad (2.3a)$$

$$= \tfrac{1}{2} \quad (h=\text{pion})\,. \qquad (2.3b)$$

Because we do recognize the different charges of u- and d-type valons (to be labeled U and D, respectively), $\mathcal{F}^v$ does depend on v.

By the convolution theorem, (2.1) implies the moment equation

$$M^h(n,Q^2)=\sum_v M_{v/h}(n)M^v(n,Q^2)\,, \qquad (2.4)$$

where

$$M^{h,v}(n,Q^2)=\int_0^1 dx\, x^{n-2}\mathcal{F}^{h,v}(x,Q^2)\,, \qquad (2.5)$$

$$M_{v/h}(n)=\int_0^1 dy\, y^{n-1}G_{v/h}(y). \qquad (2.6)$$

If we use $M_3(n,Q^2)$ to denote the average of the moments of $xF_3(x,Q^2)$ for νN and $\bar{\nu}N$ scattering on isoscalar target, we can obtain[13] from (2.4) with $\theta_C=0$,

$$M_3(n,Q^2)=3M_{v/N}(n)M^v_{\rm NS}(n,Q^2)\,, \qquad (2.7)$$

where $M^v_{\rm NS}$ is the nonsinglet (NS) component of the moment of quark distribution in a valon. Equation (2.7) is of the form of the solution of the renormalization-group equation, viz., a product of an uncalculable coefficient ($M_{v/N}$) and a function ($M^v_{\rm NS}$) calculable in QCD, especially at high Q^2. Since M_3 is measured in recent neutrino experiments, $M_{v/N}$ can be determined from (2.7) using QCD results. An equation similar to (2.7) can also be derived for muon scattering. If flavor independence is not assumed, simultaneous analysis of both ν and μ data can then lead to a separation of the U and D valon distributions and their moments.

Recall now our earlier remark that the right-hand side of (2.1) has an implicit dependence on Q_v. At Q_v, $\mathcal{F}^v(z,Q_v^2)$ is proportional to $\delta(z-1)$,

signifying that a valon behaves as a constituent quark with no internal structure that can be resolved at Q_v. QCD supplemented by this boundary condition completely defines a valon. The implication of the boundary condition on the moments is

$$M_{\rm NS}^{v}(n,Q_v^2)=1. \tag{2.8}$$

At high Q^2 the solution of the renormalization-group equation has the simple form

$$M_{\rm NS}^{v}(n,Q^2)=\left(\frac{\alpha(Q^2)}{\alpha(Q_v^2)}\right)^{d_n^{\rm NS}}, \tag{2.9}$$

where in leading-logarithm approximation

$$\alpha(Q^2)=\frac{12\pi}{(33-2f)\ln Q^2/\Lambda^2}, \tag{2.10}$$

f being the number of flavors, Λ the scale of strong interactions, and $d_n^{\rm NS}$ the NS anomalous dimension

$$d_n^{\rm NS}=\frac{4}{33-2f}\left(1-\frac{2}{n(n+1)}+4\sum_{j=2}^{n}\frac{1}{j}\right).$$

At low Q^2, (2.10) is invalid; consequently, it cannot be applied for the evaluation of $\alpha(Q_v^2)$ in (2.9). Furthermore, (2.9) itself becomes inaccurate and must be supplemented by other nonleading terms. It means that $[M_{\rm NS}^{v}(n,Q^2)]^{-1/d_n^{\rm NS}}$, though proportional to $\ln Q^2$ at high Q^2, deviates from a straight line in a logarithmic plot at low Q^2 and approaches one at Q_v^2. This is illustrated in Fig. 2. Since the theoretical understanding of the low-Q^2 behavior is incomplete at present, we shall circumvent the difficulty associated with it in the following way. First, we emphasize that the linear part of Fig. 2 is what we want to exploit in the following. The boundary condition (2.8) at Q_v^2, however, cannot be applied unless we follow the nonlinear curve at low Q^2. Now, if we stay on the linear line and extrapolate, we would arrive at a different value (Q_0^2), where the extrapolated moments are unity. Thus as far as the linear portion goes, we can just as well use the effective formula

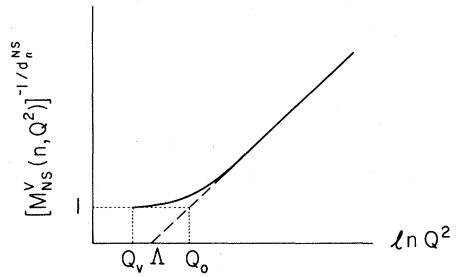

FIG. 2. Sketch of the behavior of $[M_{\rm NS}^{v}(n,Q^2)]^{-1/d_n^{\rm NS}}$ as a function of $\ln Q^2$. The solid line indicates how it might deviate from a straight line when Q^2 is low. The dashed line is a linear extrapolation. The two lines have the boundary value of one at Q_v and Q_0, respectively.

$$[M_{\rm NS}^{v}(n,Q^2)]^{-1/d_n^{\rm NS}}=\frac{\ln Q^2/\Lambda^2}{\ln Q_0^2/\Lambda^2}. \tag{2.11}$$

The role of Q_0 here is essentially to parametrize the slope of the linear line in Fig. 2 and should not be regarded as having anything to do with (2.10). It can be interpreted as an effective value of Q where $M_{\rm NS}^{v}(n,Q^2)=1$, provided that the moments are approximated by the leading-order result. Thus in that approximation the Q^2 evolution starts at Q_0^2. Because (2.10) is not used, there is no reason why Q_0 cannot be very close to Λ. It can also be interpreted as giving a rough estimate of the effective size of a valon. It is important to recognize that Q_0 is not an arbitrary parameter chosen to be large enough to justify leading-order calculation. It has a physical meaning, and its value can be determined phenomenologically.

While $M_{\rm NS}^{v}(n,Q^2)$ is a theoretical quantity that cannot be measured directly, $M_3(n,Q^2)$ is the moment of experimentally determined structure function. Combining (2.7) and (2.11) we now have for large Q^2

$$[M_3(n,Q^2)]^{-1/d_n^{\rm NS}}=S(n)\ln Q^2/\Lambda^2, \tag{2.12}$$

where

$$S(n)=[3M_{v/N}(n)]^{-1/d_n^{\rm NS}}/\ln(Q_0^2/\Lambda^2). \tag{2.13}$$

The linear dependence on $\ln Q^2/\Lambda^2$ in (2.12) has been verified by neutrino experiments[21-23] and is regarded as a successful test of QCD. The data of Refs. 21 and 22, however, have apparent discrepancies when the quantity in (2.12) is plotted against $\ln Q^2$. They are due largely to the use of different values of f in the evaluation of $d_n^{\rm NS}$. In Ref. 13 we used BEBC-Gargamelle data[21] and obtained the following results (for $f=3$):

$$\Lambda=0.74\ \text{GeV},\quad Q_0=0.82\ \text{GeV}, \tag{2.14}$$

$$G_{v/N}(y)=\tfrac{105}{16}y^{1/2}(1-y)^2. \tag{2.15}$$

The method used there depends crucially on the availability of the $n=2$ moment, for which we know from (2.3) that $M_{v/N}(2)=\frac{1}{3}$. Since the CERN-Dortmund-Heidelberg-Saclay (CDHS) data[22,23] do not provide $M_3(2,Q^2)$, we use here a slight variation of the method to extract $G_{v/N}(y)$. Adopting $f=3$ as being more relevant, we plot $[M_3(n,Q^2)]^{-1/d_n^{\rm NS}}$ against $\ln Q^2$ as in Fig. 3 and obtain $\Lambda^2=0.3\ \text{GeV}^2$. The slopes $S(n)$ of the straight-line fits are then determined, as shown in Fig. 4. To fit $S(n)$, we assume that the valon distribution has the form

$$G_{v/N}(y)=g_0y^{j-1}(1-y)^{k-1}, \tag{2.16}$$

in which the three parameters are constrained by (2.2) and (2.3), i.e.,

$$g_0=[B(j,k)]^{-1},\quad j=\tfrac{1}{2}k, \tag{2.17}$$

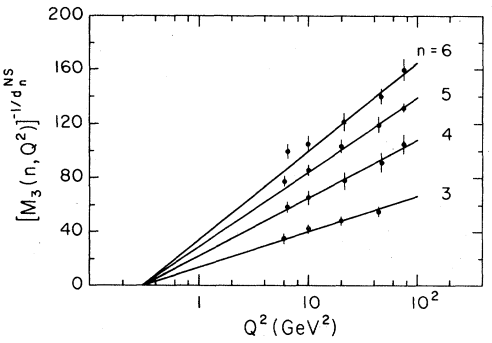

FIG. 3. Plot of $[M_3(n, Q^2)]^{-1/d_n^{NS}}$ versus Q^2 for various moments. Points are obtained by analyzing data in Refs. 22 and 23 using $f=3$. Straight lines are eyeball fits through $\Lambda^2=0.3$ GeV^2.

where $B(j,k)$ is the beta function. Thus the moments of (2.16) are

$$M_{v/N}(n)=B(n+\tfrac{1}{2}k-1,k)/B(\tfrac{1}{2}k,k)\,. \tag{2.18}$$

We can then fit $S(n)$ by (2.13) and (2.18), treating Q_0 and k as free parameters. The results are shown in Fig. 4. The best fit (solid line) is for

$$k=2.5,\ Q_0=0.65\ \text{GeV},\ \Lambda=0.55\ \text{GeV}, \tag{2.19a}$$

although a fit with $k=3$ (dashed line) is also in good agreement with the data; the parameters are

$$k=3.0,\ Q_0=0.64\ \text{GeV},\ \Lambda=0.55\ \text{GeV}. \tag{2.19b}$$

The difference between (2.14) and (2.19) reflects the discrepancies between the data of Refs. 21 and 22. Nevertheless, if we regard the range of k from 2.5 to 3.0 to be adequately approximated by the value 3, then both sets of data yield the same valon distribution, i.e., (2.15), which is not sensitive to the absolute normalization of the data. We have

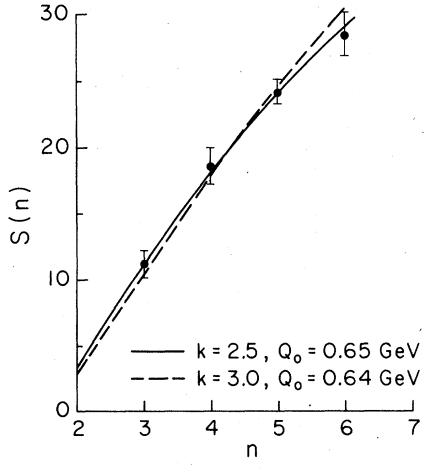

FIG. 4. Slope parameter $S(n)$ as determined from Fig. 3. The two curves represent two possible fits, using Eqs. (2.13) and (2.18).

therefore extracted a rather essential feature of the data. It describes the wave function of the valons inside a nucleon. It summarizes the hadronic structure—the part that is not calculable by present methods in QCD.

While (2.15) is obtained by detailed analyses of the deep-inelastic scattering data, the result can also be obtained by an alternative and more direct method, once the reality of the valon concept is accepted. The only experimental input needed is that $\nu W_2 \sim (1-x)^3$ as $x\to 1$. Since k is the only parameter to be determined in (2.16), we need only examine the large-x, hence large-y behavior of (2.1). The information we need from QCD is the large-z behavior of the valon structure function $\mathcal{F}^v(z,Q^2)$ at moderate Q^2. We have already mentioned that this function has the boundary condition that it is proportional to $\delta(z-1)$ at Q_v^2. At higher Q^2 gluon bremsstrahlung smooths out this singularity at $z=1$ and turns $\mathcal{F}^v(z,Q^2)$ into a gently varying function of z, the shape of which depends on Q^2. But for any Q^2 not too close to Q_v^2 the universal feature is that $\mathcal{F}^v(z,Q^2)$ is finite as $z\to 1$.[20] Using this property in (2.1) implies at moderate Q^2

$$\mathcal{F}^N(x)\propto \int_x^1 dy\, G_{v/N}(y),\quad x\to 1\,. \tag{2.20}$$

Hence, the experimental fact that the left-hand side behaves as $(1-x)^3$ demands the $(1-y)^2$ behavior for the integrand as $y\to 1$. The distribution in (2.15) then follows uniquely, given (2.16) and (2.17). At high enough Q^2, $\mathcal{F}^v(z,Q^2)$ will vanish as $z\to 1$; the consequence on $\mathcal{F}^N(x,Q^2)$ is then that it will vanish faster than $(1-x)^3$ by a corresponding increase in the exponent completely determined by (2.1). This is the expected result in QCD. At low or medium Q^2 there is no such complication, and the general result from (2.20) is that for any hadron h we have

$$G_{v/h}(y)\propto(1-y)^{k-1},\ \text{as } y\to 1\,, \tag{2.21}$$

if and only if

$$\mathcal{F}^h(x)\propto(1-x)^k,\ \text{as } x\to 1\,. \tag{2.22}$$

Obviously, this method can be applied to the meson case where only the large-x behavior is known.

Consider now the valon distribution in a pion. The momentum sum rule (2.3b) implies $j=k$, so it follows that

$$G_{v/\pi}(y)=\frac{1}{B(k,k)}[y(1-y)]^{k-1}\,. \tag{2.23}$$

There is now reasonably good evidence from massive-lepton-pair production[24] that the structure function of a pion behaves very nearly like $(1-x)^1$ as $x\to 1$. From (2.22) and (2.23) this means $k=1$

and

$$G_{v/\pi}(y)=1\,. \tag{2.24}$$

Similar consideration when applied to the K meson would give the same result if the structure function of a kaon behaves also as $(1-x)^1$. However, we can do better than that. Since a valon plays the role of a constituent quark, the strange and nonstrange valons should have different masses, and therefore different momentum distributions. We shall consider this problem below after discussing the multivalon distributions.

Since we know the precise number of valons in a hadron, and since we do not distinguish valon types of the same mass, the multivalon distributions can be simply obtained by symmetry consideration and sum rules. Consider first the nucleon case. We write the three-valon distribution in the general symmetric form

$$G_{v/N}(y_1,y_2,y_3)=\alpha_N(y_1y_2y_3)^{\kappa-1}\delta(y_1+y_2+y_3-1)\,. \tag{2.25}$$

Then the two-valon distribution is

$$\begin{aligned}G_{v/N}(y_1,y_2)&=\int_0^1 dy_3 G_{v/N}(y_1,y_2,y_3)\\&=\alpha_N[y_1y_2(1-y_1-y_2)]^{\kappa-1}\end{aligned} \tag{2.26}$$

and the single-valon distribution is

$$\begin{aligned}G_{v/N}(y_1)&=\int_0^{1-y_1} dy_2 G_{v/N}(y_1,y_2)\\&=\alpha_N B(\kappa,\kappa)y_1^{\kappa-1}(1-y_1)^{2\kappa-1}\,.\end{aligned} \tag{2.27}$$

Comparing this with (2.15) yields

$$\kappa=3/2,\quad \alpha_N=105/2\pi\,. \tag{2.28}$$

Note that (2.26) specifies how the distribution vanishes as $y_1+y_2\to 1$. It will play an important role in a later section in determining the limiting behavior of the two-parton distribution $F(x_1,x_2)$ and in avoiding the assumption of either the factorizable form (1.3) or the Kuti-Weisskopf model.[7]

In the pion case the two-valon distribution is

$$G_{v/\pi}(y,y_2)=\alpha_\pi(y_1y_2)^{\lambda-1}\delta(y_1+y_2-1)\,. \tag{2.29}$$

Integration over y_2 and comparison with (2.24) yield

$$\alpha_\pi=1,\quad \lambda=1\,. \tag{2.30}$$

For kaons, we take into account the mass difference between light and heavy valons, identifying the former with the nonstrange constituent quarks, and the latter with the strange constituent quark. We write the two-valon distribution in a kaon as

$$G_{v/K}(y_1,y_2)=\alpha_K y_1^{a-1}y_2^{b-1}\delta(y_1+y_2-1)\,, \tag{2.31}$$

where y_1 is the momentum fraction of the light valon and y_2 that of the heavy one. The single-valon distributions are then

$$G_{v_l/K}(y_1)=\alpha_K y_1^{a-1}(1-y_1)^{b-1}\,, \tag{2.32a}$$

$$G_{v_h/K}(y_2)=\alpha_K y_2^{b-1}(1-y_2)^{a-1}\,, \tag{2.32b}$$

where $\alpha_K=[B(a,b)]^{-1}$. The average momentum fractions carried by the light and heavy valons are, respectively.

$$\bar{y}_1=\alpha_K B(a+1,b)=a/(a+b), \tag{2.33a}$$

$$\bar{y}_2=\alpha_K B(a,b+1)=b/(a+b)\,. \tag{2.33b}$$

If we regard the valons as constituent quarks bound nonrelativistically in a bag, then their average momenta should be proportional to their masses, m_l and m_h. Thus we have

$$\frac{a}{b}=\frac{\bar{y}_1}{\bar{y}_2}=\frac{m_l}{m_h}\simeq\frac{2}{3}\,. \tag{2.34}$$

With this constraint it should be possible to determine a and b separately by fitting data on lepton-pair production in kaon-initiated reactions using the Drell-Yan model,[25] or by applying the recombination model to low-p_T inclusive reactions involving K mesons.[26]

Similar consideration can be applied to the hyperon in determining the effect of valon mass difference on the momentum distribution. Adopting the form

$$G_{v/Y}(y_1,y_2,y_3)=\alpha_Y(y_1y_2)^{a-1}y_3^{b-1}\delta(y_1+y_2+y_3-1) \tag{2.35}$$

for the three-valon distribution, where y_1 and y_2 refer to the two light valons, and y_3 the heavy one, one can show that

$$\alpha_Y=[B(a,a+b)B(a,b)]^{-1} \tag{2.36}$$

and

$$\frac{a}{b}=\frac{m_l}{m_h}\simeq\frac{2}{3}\,. \tag{2.37}$$

We have thus far dwelt exclusively on the distribution functions $G_{v/h}(y)$, etc., which are probability functions defined in the noninvariant phase space dy. The invariant distributions defined in the invariant phase space dy/y are

$$F_{v/h}(y)=yG_{v/h}(y)\,, \tag{2.38a}$$

$$F_{v/\pi}(y_1,y_2)=y_1y_2G_{v/\pi}(y_1,y_2)\,, \tag{2.38b}$$

$$F_{v/N}(y_1,y_2,y_3)=y_1y_2y_3G_{v/N}(y_1,y_2,y_3)\,, \tag{2.38c}$$

etc. Sometimes it is more convenient to work with the F rather than the G functions. One can readily keep track of all the momentum factors in a convolution equation if all quantities are invariant F and integrals are performed over the invariant

phase space.

It should be noted that the valon distributions derived here are extracted from data at values of x not in the extreme $x \to 1$ limit. For example, the moments in Fig. 3 are for $n \leq 6$. Consequently, the expressions for the valon distributions, though reliable for the bulk of the y range, may not be very accurate when y is extremely close to 1. The inadequacy may be more than a matter of data analysis. In the extreme $x \to 1$ limit the quark probed is far off-shell,[17,18] and the exact QCD prediction[27] for the x distribution in that limit differs from our result on the large-y behavior. Of course, they should not be compared directly. The valons are clusters at low Q^2 and are not ever far off-shell. Their relationship to the quarks that are far off-shell very near $x = 1$ is at present unclear and deserves further attention.

III. RECOMBINATION FUNCTION

When the recombination functions was first introduced[3] there was some uncertainty about its precise form. For the formation of a meson, quark-antiquark recombination was considered dominant. The gluons would contribute to multiparton recombination processes, which were though to be less important. On the basis of the counting rule the momentum dependence of the recombination function was suggested to be that given in (1.2). The normalization constant α was unspecified. The important property of (1.2) is that it vanishes at $x_i = 0$ and 1, signifying short-range correlation. Indeed, it has been shown[9] that (1.2) corresponds to a correlation length of two units in rapidity. Although the phenomenological application of (1.2) has been successful, the recombination function has thus far remained as an imprecisely defined quantity, and its derivation lacks rigor. A better understanding of this function is crucial to a proper formulation of the recombination model.

The task is made simple by the development of the valon concept. Take the pion for definiteness. The absolute square of the wave function $\langle v_1(y_1)v_2(y_2)|\pi\rangle$ describes not only the probability of finding the two valons of a pion at y_1 and y_2, but also the probability of forming a pion from two valons at those y_i values. The amplitudes are related by complex conjugation. In a theory in which valon states are defined, this relationship is exact and defines recombination. Thus the invariant recombination function is

$$R^{\pi}(y_1,y_2) = F_{v/\pi}(y_1,y_2) . \tag{3.1}$$

The reason why we have no ambiguity here, as opposed to the case in Ref. 3, is that the valon content of a hadron is definite and known. Gluons are automatically taken into account in that they dress up the quarks to form the valons. The question of how the partons in an incident hadron turn into valons of the produced particles remains to be discussed, as we shall do in the next two sections. The issues are, however, distinct. Here, we are concerned only with the probability for recombination, given the valon momenta.

Equation (3.1) expresses the recombination function when the pion momentum is normalized to one. If the pion momentum is a fraction x of the initial hadron momentum, then (2.29), (2.30), (2.38b), and (3.1) imply

$$R^{\pi}(x_1,x_2,x) = \frac{x_1 x_2}{x^2}\,\delta\!\left(\frac{x_1}{x}+\frac{x_2}{x}-1\right) , \tag{3.2}$$

in agreement with (1.2). Moreover, the normalization is now completely fixed. Note that x_1 and x_2 refer to the momentum fractions of the valons that recombine. The result is obtained without using the counting rule,[4] yet it is in agreement with that obtained by using it, provided that quarks are replaced by valons. In a similar way we can get the recombination functions for the other hadrons:

$$\text{kaon: } R^{K}(x_1,x_2,x) = [B(a,b)]^{-1}\left(\frac{x_1}{x}\right)^{a}\left(\frac{x_2}{x}\right)^{b}\delta\!\left(\frac{x_1}{x}+\frac{x_2}{x}-1\right) , \tag{3.3}$$

$$\text{nucleon: } R^{N}(x_1,x_2,x_3,x) = \frac{105}{2\pi}\left(\frac{x_1 x_2 x_3}{x^3}\right)^{3/2}\delta\!\left(\frac{x_1}{x}+\frac{x_2}{x}+\frac{x_3}{x}-1\right) , \tag{3.4}$$

$$\text{hyperon: } R^{Y}(x_1,x_2,x_3,x) = \frac{(x_1x_2/x^2)^{a}(x_3/x)^{b}\delta\!\left(\frac{x_1}{x}+\frac{x_2}{x}+\frac{x_3}{x}-1\right)}{B(a,a+b)B(a,b)} . \tag{3.5}$$

IV. QUARK DECAY FUNCTION

Before we consider the problem of hadron fragmentation, we discuss first quark fragmentation as an introduction to the subject. The decay function for quark fragmentation can be calculated exactly in QCD and the recombination model without

using any phenomenological input, and the result gives a good no-parameter fit to the data.[12] The decay function $D(x,Q^2)$ is related to the $q\bar{q}$ distribution and recombination function in just the same way as in (1.1):

$$xD(x,Q^2)=\int F(x_1,x_2,Q^2)R(x_1,x_2,x)\frac{dx_1}{x_1}\frac{dx_2}{x_2}\,, \tag{4.1}$$

except that now the F function depends also on Q^2, which in the case of a quark jet from e^+e^- annihilation, for example, is the square of the c.m. energy. When Q^2 is large, $F(x_1,x_2,Q^2)$ can be calculated in QCD. Hadron fragmentation is difficult to treat precisely because $F(x_1,x_2)$ in (1.1) has no large Q^2, so perturbative method in QCD is not applicable. Nevertheless, the similarity between (1.1) and (4.1) provides us with the opportunity to use quark fragmentation as a more tractable example to elucidate the ideas involved in our calculation of hadron fragmentation in Sec. V.

A pictorial depiction of (4.1) is shown in Fig. 5. The crosshatched blobs represent evolution functions which describe the degradation of Q^2 as the quark created at the virtual-photon vertex emits gluons and quark pairs. $F(x_1,x_2,Q^2)$ is the $q\bar{q}$ distribution represented by the part in the figure from the initial quark at Q^2 to the q and $\bar{q}$ at the position of the vertical dotted line. Evidently, one bifurcation vertex must be considered explicitly, at which the momentum fractions and virtual masses of the quarks and gluons involved are to be integrated and the parton types (quark, antiquark, and gluons) are to be summed. The evolution functions are known from renormalization-group analysis. On the other side of the dotted line in Fig. 5 is the recombination function. At the dotted line the Q^2 value associated with the q and $\bar{q}$ is Q_0^2. It may appear inconsistent to regard them on the one hand as quark and antiquark resulting from sequential bifurcations in $F(x_1,x_2,Q^2)$, but on the other hand as valons in connection with hadronization through $R(x_1,x_2,x)$, the label Q_0^2 being implicit in both these functions. This duality is actually an essential property of the valons since they play the role of bridging the hard and soft processes. What is involved is exactly analogous to the case of structure functions for which the valon concept was first introduced, the only difference being the direction of Q^2 change. Recall (2.1) and Fig. 1. In the two factors in the integrand, or for the two blobs in Fig. 1, the valon plays dual roles. In $G_{v/h}(y)$ the valon is the valence-quark cluster, and at Q_0 its internal structure cannot be discerned. The counterpart of $G_{v/h}(y)$ in (4.1) is $R(x_1,x_2,x)$, the precise connection having been established by (3.1). For the factor $\mathcal{F}^v(z,Q^2)$ in (2.1) describing the structure function of a valon, the mathematical treatment regards the valon initially as a point quark at Q_0 with momentum distribution $\delta(z-1)$, and tracks the modification of the distribution as a result of gluon bremsstrahlung until a quark in the cluster is struck by a virtual photon at Q^2. This is done in QCD with the initial and final quarks treated as point quarks. Loosely, one may refer to the distribution as quark structure function,[20] but physically it is the valon structure function. The counterpart of $\mathcal{F}^v(z,Q^2)$ in (4.1) is $F(x_1,x_2,Q^2)$. Evidently, the processes represented by Figs. 1 and 5 are analogous; in the former, Q^2 increases from left to right, while in the latter, it decreases.

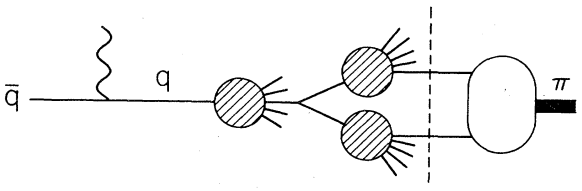

FIG. 5. A schematic diagram showing pion production in a quark jet initiated by a virtual photon. The three shaded blobs represent inclusive parton (quark, antiquark, or gluon) distributions in partons. The open blob represents recombination.

The parallel between (2.1) and (4.1) provides the excuse for the use of leading-order calculation of $F(x_1,x_2,Q^2)$ in perturbative QCD for Q^2 degradation all the way down to Q_0^2. That is because Q_0 itself is determined in the same approximation. Recall that it is with the leading-order result for $\mathcal{F}^v(x/y,Q^2)$ substituted into (2.1) that the νN data is fitted. Thus, in both the structure function $\mathcal{F}^h(x,Q^2)$ and the decay function $xD(x,Q^2)$, the leading-order approximation (and the associated choice of Q_0) is the common vehicle that is convenient in relating valons to hard-collision processes. An improvement of the approximation does not change the parallelism in those relationships for the two functions, nor is it likely to lead to a significantly different result for $D(x,Q^2)$ if the structure function is regarded as the source of phenomenological input on the degree of evolution.

A final remark about the calculation of $D(x,Q^2)$ is that it must account for the momenta carried by the gluons because hadronization is complete, i.e., all partons get converted into hadrons in the end. If $F(x_1,x_2,Q^2)$ is the $q\bar{q}$ inclusive distribution in a quark jet which has momentum leakage into the gluons, its use in (4.1) would not lead to the correct normalization for $D(x,Q^2)$. Thus it is necessary to include in $F(x_1,x_2,Q^2)$ the q and $\bar{q}$ con-

verted from gluons. In that way the recombination model can fully account for the hadronization of all the partons in the quark jet.

All the considerations about quark fragmentation discussed in this section have their counterparts in hadron fragmentation to which we now turn.

V. HADRON FRAGMENTATION

The problem of hadron fragmentation is difficult to treat because, unlike hard-collision processes, it has no large Q^2 scale. Hadron-hadron collisions at high energies are dominantly soft processes since reaction rates drop precipitously with increasing p_T. Thus they do not reflect the short-distance behavior of the interaction, and one cannot use the usual impulse approximation valid for large-Q^2 reactions. However, there is one feature about multiparticle production that saves us from hopeless complications. It is the short-range correlation of the produced particles. On the basis of that one may first of all be justified to ignore the target hadron when studying the fragmentation region of the projectile. Furthermore, at the parton level the interaction between partons must also be short-ranged. The recombination model relies on the short-range character of the interaction to describe the hadronization process which is approximately local in rapidity ($\Delta y \sim 2$) so that what goes on in the fragmentation region may be dissociated from that in the central region. These properties form the basis for (1.1), which has an appearance that follows from impulse approximation.

What is involved in hadron fragmentation is a multistage process:

$$\text{initial hadron} \xrightarrow{(1)} \text{valons} \xrightarrow{(2)} \text{partons} \xrightarrow{(3)} \text{valons} \xrightarrow{(4)} \text{produced hadrons}. \tag{5.1}$$

Stage (1) has been discussed in Sec. II and is represented by the valon distribution $G_{v/h}$. Stage (4) is known from Sec. III and is described by the recombination function R. Stages (2) and (3) are our concerns here; together with (1) they specify $F(x_1,x_2)$, which is the major unknown in (1.1).

A. Stage (2)

If we were able to peek at the parton state without disturbing the system, we would presumably discover quark and antiquark distributions which are very close to the ones determined by electroproduction at low Q^2. We do not know how low the value of Q^2 must be in order to be relevant to the low-p_T problem. In the precursor model for $F(x_1,x_2)$, which denoted two-parton distribution since the valon concept was not yet introduced, the form (1.3) was adopted,[3] where $F_q(x_1)$ and $F_{\bar{q}}(x_2)$ were assumed to be the quark and antiquark distributions determined by Field and Feynman[28] in fitting the SLAC data on nucleon structure functions. The Q^2 range was 1–5 GeV^2. Although one may question whether such "high" values of Q^2 are relevant for low-p_T reactions where $p_T^2 \ll 1$ (GeV/c)^2, the result of the calculation lends support to their relevance. Presumably, precocious scaling implies that the precise value of Q^2 is unimportant and that even at Q^2 in the vicinity of 3 GeV^2 the parton distributions have already run through the major course of their Q^2 changes (i.e., mature evolution). Indeed, as we shall see below, the parameter that characterizes the evolution from valons to partons in stage (2) turns out to be quite large.

The strategy of our approach to the problem is as follows. We first admit that we have no way to calculate the parton distributions from first principles. Some free parameters must per force be introduced; they are, however, not to be determined by the hadronic inclusive cross section for which we want to obtain a no-parameter fit, but by $\nu W_2(x)$ at low Q^2. What we achieve as an improvement over (1.3) is that the valon distribution in stage (1) properly introduces the hadron wave function and automatically takes care of the phase-space problem, which was handled in an *ad hoc* manner by the factor $\rho(x_1,x_2)$ in (1.3). The evolution in stage (2) from the valons to the partons will be parametrized by formulas reminiscent of QCD. Although they cannot be taken seriously, the largeness of the evolution parameter renders the procedure not totally nonsensical.

For definiteness we shall consider hereafter the fragmentation of the proton only and the detection of π^+ in particular. Thus a valence u quark in the proton ends up in the π^+. Let $\Phi(x_1,x_2)$ be the invariant inclusive distribution of u and $\bar{d}$ carrying momentum fractions x_1 and x_2 of the proton, respectively. It is obtained by a convolution of the distributions in stages (1) and (2). Since the u and $\bar{d}$ quarks may either both come from the same valon or come separately from two different valons, $\Phi(x_1,x_2)$ has two components

$$\Phi(x_1,x_2) = \Phi^{(1)}(x_1,x_2) + \Phi^{(2)}(x_1,x_2), \tag{5.2}$$

which are illustrated by the diagrams in Fig. 6. Let $K(z)$ denote the invariant distribution of finding

a quark with momentum fraction z in a valon of the same flavor. (As in all distributions considered in this paper, color and spin components are averaged over in the initial state and summed in the final state so that we are not concerned explicitly with such degrees of freedom.) Let $L(z)$ be the same for any antiquark or a quark with flavor different from that of the parent valon. Since a proton has two U valons and one D valon, we have

$$\Phi^{(1)}(x_1,x_2)=2\int dy\, G_{U/N}(y)\,\tfrac{1}{2}\left[K\left(\frac{x_1}{y}\right)L\left(\frac{x_2}{y-x_1}\right)+L\left(\frac{x_2}{y}\right)K\left(\frac{x_1}{y-x_2}\right)\right]+\int dy\, G_{D/N}(y)L\left(\frac{x_1}{y}\right)L\left(\frac{x_2}{y-x_1}\right), \tag{5.3}$$

$$\Phi^{(2)}(x_1,x_2)=2\int dy_1dy_2G_{UU/N}(y_1,y_2)K\left(\frac{x_1}{y_1}\right)L\left(\frac{x_2}{y_2}\right)+2\int dy_1dy_2G_{UD/N}(y_1,y_2)\left[K\left(\frac{x_1}{y_1}\right)+L\left(\frac{x_1}{y_1}\right)\right]L\left(\frac{x_2}{y_2}\right). \tag{5.4}$$

In our approximation in Sec. II, the valon distributions are assumed to be flavor independent due to the lack of high-Q^2 data from which to extract the flavor dependence. Thus for brevity we shall suppress the subscripts of the G functions in (5.3) and (5.4), and in computation below use (2.27) and (2.26) for them, respectively.

Equation (5.3) is not precisely a convolution equation. The distribution of $u\bar{d}$ in a valon is analogous to that in a quark jet, for which a precise expression in perturbative QCD is given in Ref. 12. But at low Q^2 such an expression for a valon jet is unreliable. Since the functions K and L will be determined phenomenologically anyway, an approximate expression such as the one in (5.3) that captures the essence of quark jets is totally adequate. The u quark and $\bar{d}$ antiquark distributions in a proton are, respectively,

$$\Phi_u(x)=\int_x^1 dy\, G(y)\left[2K\left(\frac{x}{y}\right)+L\left(\frac{x}{y}\right)\right] \tag{5.5}$$

and

$$\Phi_{\bar{d}}(x)=3\int_x^1 dy\, G(y)L\left(\frac{x}{y}\right). \tag{5.6}$$

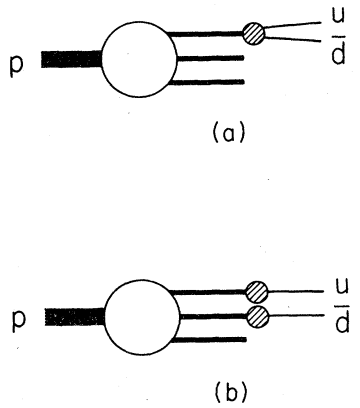

FIG. 6. Schematic diagrams for (a) $\Phi^{(1)}(x_1, x_2)$, where u and $\bar{d}$ quarks come from the same valon and (b) $\Phi^{(2)}(x_1, x_2)$, where they come from different valons.

Relationships between $\Phi(x_1,x_2)$ and $\Phi(x)$ such as

$$\int_0^{1-x_1}\frac{dx_2}{x_2}\,\Phi(x_1,x_2)=\langle n(x_1)\rangle\Phi(x_1) \tag{5.7a}$$

should not play an important role since the x_1 dependence of $\langle n(x_1)\rangle$, which is the parton multiplicity associated with a parton at x_1, is unknown; besides, its magnitude is infinite in the strict scaling limit. Similarly, momentum sum rule

$$\int_0^{1-x_1}dx_2\Phi(x_1,x_2)=\langle x_2(x_1)\rangle\Phi(x_1) \tag{5.7b}$$

is not useful as an extra constraint on the relationship between $\Phi(x_1,x_2)$ and $\Phi(x_1)$ because $\langle x_2(x_1)\rangle$ is not known *a priori*, it being the average total momentum fraction of parton 2 associated with a parton at x_1. Equations (5.2)–(5.4) provide a basic improvement over (1.3). In our view they constitute a physically more correct expression of the two-parton distribution than the Kuti-Weisskopf model.[7]

The functions $K(z)$ and $L(z)$ are to be determined by ensuring that they lead to the correct Φ_u and $\Phi_{\bar{d}}$ distributions at low Q^2. More precisely, we calculate the observable quantities $\nu W_2(x)$ and the sea quark distribution $xS(x)$ which can be determined from leptoproduction data:

$$\begin{aligned}\nu W_2(x)&=\int dy\,2G_{U/p}(y)\left\{\frac{4}{9}\left[K\left(\frac{x}{y}\right)+L\left(\frac{x}{y}\right)\right]+\frac{1}{9}\left[4L\left(\frac{x}{y}\right)\right]\right\}\\&\quad+\int dy\,G_{D/p}(y)\left\{\frac{4}{9}\left[2L\left(\frac{x}{y}\right)\right]+\frac{1}{9}\left[K\left(\frac{x}{y}\right)+3L\left(\frac{x}{y}\right)\right]\right\}\\&=\int dy\,G(y)\left[K\left(\frac{x}{y}\right)+3L\left(\frac{x}{y}\right)\right],\end{aligned} \tag{5.8}$$

$$\begin{aligned}xS(x)&=\int dy\left[2G_{U/p}(y)L\left(\frac{x}{y}\right)+G_{D/p}(y)L\left(\frac{x}{y}\right)\right]\\&=3\int dy\,G(y)L\left(\frac{x}{y}\right).\end{aligned} \tag{5.9}$$

$K(z)$ and $L(z)$ are favored and unfavored distribu-

tions[20] which can be expressed in terms of the singlet (K_S) and nonsinglet (K_{NS}) components:

$$K=[K_S+(2f-1)K_{NS}]/2f=K_{NS}+L\ , \tag{5.10}$$

$$L=(K_S-K_{NS})/2f\ . \tag{5.11}$$

Hence, we can rewrite (5.8) as

$$\nu W_2(x)=\int dy\, G(y)\left[K_{NS}\left(\frac{x}{y}\right)+4L\left(\frac{x}{y}\right)\right]. \tag{5.12}$$

Now, we specify the parametrization of the uncalculable functions $K_{NS}(z)$ and $L(z)$ so that they can be determined phenomenologically. For $K_{NS}(z)$ we assume on the basis of precocious scaling that its moments, $K_{NS}(n)$, defined as in (2.5), have a form that can be mimicked by the solution of the renormalization-group equation, i.e.,

$$K_{NS}(n)=\exp(-d_n^{NS}\zeta)\ , \tag{5.13}$$

where ζ is a free parameter to be adjusted to fit $\nu W_2(x)$. If the leading-logarithm approximation were sensible, then ζ would be identified as

$$\zeta=\ln\frac{\ln Q^2/\Lambda^2}{\ln Q_0{}^2/\Lambda^2}\ . \tag{5.14}$$

But we have no large Q^2 in the problem. For the present it is more proper to regard (5.13) merely as a one-parameter formula for the nonsinglet moments. For $L(z)$ there is no simple formula that can mimick the Q^2 evolution in QCD; we adopt the canonical form

$$L(z)=a(1-z)^c\ , \tag{5.15}$$

where a and c are to be adjusted to fit $\nu W_2(x)$ and $S(x)$. The only unknowns in the problem [viz., $K(z)$ and $L(z)$] are now reduced to three parameters, ζ, a, and c, which are to be determined outside the realm of the hadron fragmentation problem.

For the empirical expressions of $\nu W_2(x)$ we choose low-Q^2 data for proton and find in Ref. 29 a parametrization of the early but classic data taken at SLAC:

$$\nu W_2(x)=(1-x)^3[1.274+0.5989(1-x)-1.675(1-x)^2]\ . \tag{5.16}$$

For the sea quark distribution at low Q^2 we use

$$xS(x)=0.17(1-x)^9\ , \tag{5.17}$$

where the normalization is that suggested by Field and Feynman[28]; the exponent is in the range adopted by them and is also suggested by Berger[30] in fitting dimuon production data.

Instead of inverting the moments in (5.13) in order to fit (5.16) and (5.17), it is more convenient to work directly with moments. From (5.9), (5.12), (5.13), and (5.15) we have for the moments

$$\langle\nu W_2\rangle(n)=M_{\nu/N}(n)[\exp(-d_n^{NS}\zeta)+4aB(n-1,c+1)]\ , \tag{5.18}$$

$$\langle xS\rangle(n)=3aM_{\nu/N}(n)B(n-1,c+1)\ . \tag{5.19}$$

The empirical values for these moments can be trivially obtained from (5.16) and (5.17) and are plotted as dots in Fig. 7. They can be well fitted by (5.18) and (5.19) with the choice

$$\zeta=2.0,\quad a=0.08,\quad c=3.5\ , \tag{5.20}$$

as evidenced by the curves in Fig. 7. With these parameters fixed, we have completely determined the $u\bar{d}$ distribution $\Phi(x_1,x_2)$ through (5.2)–(5.4).

We note that the value $\zeta=2$ determined phenomenologically above turns out to be quite reasonable, if we use (5.14) to find the corresponding value of Q^2. For Q_0 and Λ given in (2.14) (derived from BEBC data[21]) and (2.19b) (from CDHS data[22,23]), we obtain $Q=1.58$ GeV and 1.69 GeV, respectively. These are just the values relevant to the data. Admittedly, (5.13) and (5.14) cannot be taken seriously for these low-Q^2 values. But the largeness of ζ (for a log log function) may render their application meaningful. It means that evolution has been substantial, a circumstance which we have already anticipated on the basis of precocious scaling and large momentum fraction for the gluons. The place in our simple formalism (in the

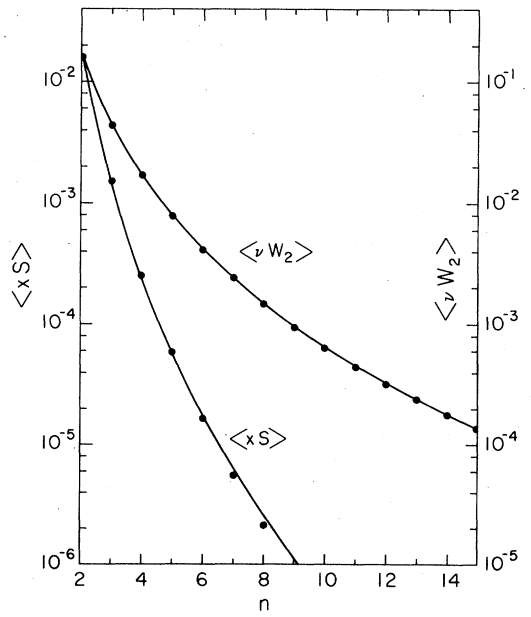

FIG. 7. Moments of νW_2 and xS. Dots are empirical values. Curves are theoretical fits that fix the parameters in the model.

sense of leading-order QCD) where such physical features at low Q^2 are stored is the closeness of Q_0 to Λ. As we have mentioned previously, Q_0 is an effective value of the evolutionary start point determined from high-Q^2 neutrino scattering data, which obviously must contain information consistent with low-Q^2 behavior.

B. Stage (3)

What we have obtained for $\Phi(x_1,x_2)$ is the inclusive distribution of u and $\bar{d}$ in proton. If they are to form a pion by recombination, the outstanding question is about the role of the gluons. Obviously, the gluons should be accounted for in some way, lest the momentum they carry would be lost from the final hadronic spectrum. In stages (3) and (4) of (5.1) we are concerned with the hadronization of all partons (including gluons), not just u and $\bar{d}$ quarks, whose distribution we have just specified. Gluons can hadronize either by being a partner of recombination with q and $\bar{q}$, or can create $q\bar{q}$ pairs which then hadronize subsequently in appropriate combinations. The former possibility implies multibody recombination which is not likely to be important except perhaps in the limit $x\to 1$; it is totally ignored in Ref. 3 as well as in other subsequent investigations. To describe it in the valon picture is also difficult. For the recombination of u and $\bar{d}$ quarks only it is easy; we simply identify them as U and $\bar{D}$ valons, which are in the proper representation for hadronization. This identification of quarks with valons is not an arbitrary approximation, but is a feature of valons, reflecting their dual properties discussed in Sec. IV. Physically, it means that the u and $\bar{d}$ quarks in time develop their own clusters and turn themselves into valons. Mathematically, the duality can be discussed more precisely in the case when there is a large Q^2, as in Sec. IV; here we simply borrow that notion without any alteration.

We are left then with the problem of hadronization of gluons through $q\bar{q}$ pair creation. This problem is treated quantitatively for a quark jet at high Q^2 because calculational method is available.[12] At low Q^2 we have no independent guidepost for the gluon distribution. Although one can make a rough estimate for it, it is not very useful if the conversion from gluons to $q\bar{q}$ pairs is not known. At this point we recall that Duke and Taylor[6] succeeded in producing a remarkably good fit of all the meson-inclusive cross sections in the recombination model by using an enhanced sea which saturates the momentum sum rule. That is, the $q\bar{q}$ sea quarks in their fit carry all the momentum of the incident proton after subtracting off the momentum fraction of the valence quarks, with none left over for the gluons. We regard that result as being a satisfactory guide to the formulation of an effective way of accounting for gluon hadronization. The gluons are first to be completely converted into $q\bar{q}$ pairs in such a way that the quiescent sea (as probed in electroproduction) is enhanced in normalization to the maximum extent with no essential change in its distribution. The valence quarks and these sea quarks are then to be regarded as valons, which recombine.

To carry out this procedure we first calculate the average momentum fraction carried by the valence quarks. It is

$$\bar{x}_v = \int dx\, x[2u(x)+d(x)]_v$$

$$= 3\int dx\,dy\, G(y) K_{\rm NS}\left(\frac{x}{y}\right)$$

$$= 3M_{v/N}(n=2)K_{\rm NS}(n=2,\xi=2) = 0.45\,. \qquad (5.21)$$

The balance in momentum fraction is carried by the enhanced sea

$$0.55 = 6\int dx\,dy\, 3G(y)\tilde{L}\left(\frac{x}{y}\right), \qquad (5.22)$$

where

$$\tilde{L}(z) = \tilde{a}(1-z)^c\,. \qquad (5.23)$$

With $c=3.5$ according to (5.20), $\tilde{a}$ is found to be 0.41. Thus the enhancement factor is about 5.

The complete $u\bar{d}$ distribution to be identified as valons at the end of stage (3) in (5.1) can now be determined. Denoting it by $F(x_1,x_2)$, we equate it to $\Phi(x_1,x_2)$ in (5.2) with the condition that $L(z)$ in (5.3), (5.4), and (5.10) be replaced by $\tilde{L}(z)$ in (5.23). That is, in the abbreviated notation of $G(y)$ and $G(y_1,y_2)$ which are flavor independent, we have

$$F(x_1,x_2) = F^{(1)}(x_1,x_2) + F^{(2)}(x_1,x_2)\,, \qquad (5.24)$$

$$F^{(1)}(x_1,x_2) = \int_{x_1+x_2}^1 dy\, G(y)\left\{\left[K_{\rm NS}\left(\frac{x_1}{y}\right)+2\tilde{L}\left(\frac{x_1}{y}\right)\right]\tilde{L}\left(\frac{x_2}{y-x_1}\right)+\tilde{L}\left(\frac{x_2}{y}\right)\left[K_{\rm NS}\left(\frac{x_1}{y-x_2}\right)+\tilde{L}\left(\frac{x_1}{y-x_2}\right)\right]\right\}, \qquad (5.25)$$

$$F^{(2)}(x_1,x_2) = 2\int_{x_1}^1 dy_1 \int_{x_2}^{1-y_1} dy_2 G(y_1y_2)\left[2K_{\rm NS}\left(\frac{x_1}{y_1}\right)+3\tilde{L}\left(\frac{x_1}{y_1}\right)\right]\tilde{L}\left(\frac{x_2}{y_2}\right). \qquad (5.26)$$

The parameters that govern K_{NS} and $\tilde{L}$ through (5.13) and (5.23) have all been fixed; they are collected here as follows:

$$\xi = 2\,, \quad \tilde{a} = 0.41\,, \quad c = 3.5\,. \tag{5.27}$$

C. Inclusive distribution for $pp \to \pi^+ X$

Since the two factors in (1.1) are now completely fixed, it is only a matter of computation to determine the inclusive cross section of the detected pion. To simplify the calculation which could involve quadruple integrals, it is best to work with moments. Denoting $(x/\sigma)(d\sigma/dx)$ by $H(x)$, we define

$$H(N) = \int_0^1 H(x) x^{N-2}\, dx\,. \tag{5.28}$$

From (1.1) and (3.2) we then obtain

$$H(N) = \sum_{m=2}^{N-1} [(m+n-3)B(m-1,n-1)]^{-1} F(m,n)\delta_{m+n,N+1} \tag{5.29}$$

for $N \geq 3$, where

$$F(m,n) = \int_0^1 dx_1 \int_0^1 dx_2 x_1^{m-2} x_2^{n-2} F(x_1,x_2) = F^{(1)}(m,n) + F^{(2)}(m,n)\,. \tag{5.30}$$

If we define the double moment transform of a function $J(z)$ by

$$J(m,n) = \int_0^1 dz\, z^{m-2}(1-z)^{n-1} J(z)\,, \tag{5.31}$$

where $J(z)$ may be either $K_{NS}(z)$ or $\tilde{L}(z)$ in (5.25), then we have in obvious notation

$$F^{(1)}(m,n) = G^{(1)}(m+n-1)\{[K_{NS}(m,n) + 2\tilde{L}(m,n)]\tilde{L}(n) + \tilde{L}(n,m)[K_{NS}(m) + \tilde{L}(m)]\}\,, \tag{5.32}$$

where

$$G^{(1)}(N) = \int_0^1 dy\, y^{N-1} G(y) = \tfrac{105}{16} B(N + \tfrac{1}{2}, 3)\,, \tag{5.33}$$

$$\tilde{L}(n) = \int_0^1 dz\, z^{n-2} \tilde{L}(z) = 0.41 B(n-1, 4.5)\,. \tag{5.34}$$

It is shown in Appendix A that

$$K_{NS}(m,n) = \sum_{k=0}^{n-1} \frac{(-1)^k}{n} [B(k+1, n-k)]^{-1} K_{NS}(m+k)\,. \tag{5.35}$$

For the moments of $F^{(2)}$ we have

$$F^{(2)}(m,n) = 2G^{(2)}(m,n)[2K_{NS}(m) + 3\tilde{L}(m)]\tilde{L}(n)\,, \tag{5.36}$$

where

$$G^{(2)}(m,n) = \int_0^1 dy_1 \int_0^{1-y_1} dy_2\, y_1^{m-1} y_2^{n-1} G(y_1, y_2) = \frac{105}{2\pi} B(m + \tfrac{1}{2}, n+2) B(n + \tfrac{1}{2}, \tfrac{3}{2})\,. \tag{5.37}$$

Using $\xi = 2$ in (5.13) all the terms above can be evaluated, so we can determine $H(N)$ unambiguously and without approximation. The result is presented as dots in Fig. 8. It is of interest to exhibit also the separate contributions of the two components, $F^{(1)}$ and $F^{(2)}$. Denoted as $H^{(1)}(N)$ and $H^{(2)}(N)$, they are shown in Fig. 8 as dashed and dash-dot lines, respectively. Evidently, the contributions from the two components are comparable, although the two-valon contribution is bigger except at high N, i.e., high x.

To invert the moments, we approximate $H(N)$ by a sum of two β functions

$$A(N) = 0.6B(N, 4.5) + 0.9B(N-1, 6)\,, \tag{5.38}$$

which is shown by the solid line in Fig. 8. It translates immediately to

$$A(x) = 0.6x(1-x)^{3.5} + 0.9(1-x)^5\,. \tag{5.39}$$

This is the theoretical prediction for $(x/\sigma_T)d\sigma/dx$ in our model without any free parameters. Using

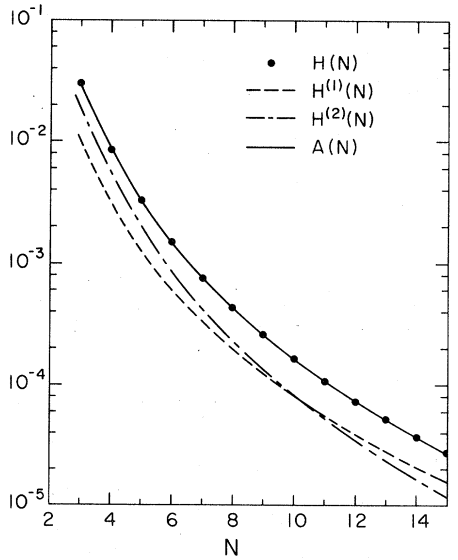

FIG. 8. Theoretical predictions for the moemnts of the hadronic inclusive distribution. Dashed and dash-dotted curves show the contributions from the two subprocesses indicated respectively in Figs. 6(a) and 6(b). The dots are their sum. The solid line represents an approximation of the dots for the purpose of inversion of the moments.

$\sigma_T = 38.7$ mb we plot the corresponding inclusive cross section in Fig. 9 (solid line). For a comparison with experiment we show in the same figure data on $pp \to \pi^+ X$ at 100 and 175 GeV.[31] The large error bars are due to the fact that the data on $Ed^3\sigma/dp^3$ must be integrated over p_T for which the measured range is not extensive. Although fixed-p_T data are abundant and of high statistics,[32-34] we need the integrated (over p_T) data in order to check the normalization as well as the shape of our prediction. The same data and theoretical result are plotted in linear scale in Fig. 10. The agreement is evidently very good over the whole x range. We emphasize that the theoretical result involves no adjustable free parameters, the only empirical input being electroproduction data.

VI. CONCLUSION

We have formulated a way of studying low-p_T reactions. Although some details may be improved, the ideas contained in the treatment probably reflect quite accurately the basic mechanism of hadron fragmentation. It is a quantitative description of what has for long been vaguely supposed for production processes in the quark model. The basic steps must involve the transitions from an incident hadron to partons and then back to hadrons. The key element in our formulation that gets rid of arbitrary constants while incorporating proper dynamics is the introduction of the valon representation. The hadronic wave function in terms of the valon coordinates is known from structure-function analysis. That takes care of the two ends of the production chain. The transmutation from valons to partons is mimicked by formulas with QCD origin, where precise parametrization is fixed by low-Q^2 electroproduction data. The part that is least reliable in the formulation is the treatment of gluon conversion. Since we know that no gluons are left over in the final state, we have adopted the classic picture that they all produce $q\bar{q}$ pairs which subsequently recombine. Thus the sea is enhanced to the maximum. Again, no free parameters are introduced if the x dependence of the enhanced sea remains the same as that of the original sea, an assumption which is not unreasonable. A similar maximal gluon-conversion mechanism is used in the quark-jet analysis but with more precision since high Q^2 is involved; the result contributes to an excellent no-parameter fit of the quark decay function.[12] In this paper we have ignored flavor dependence of the valon distribution. This should be corrected as soon as a more thorough analysis

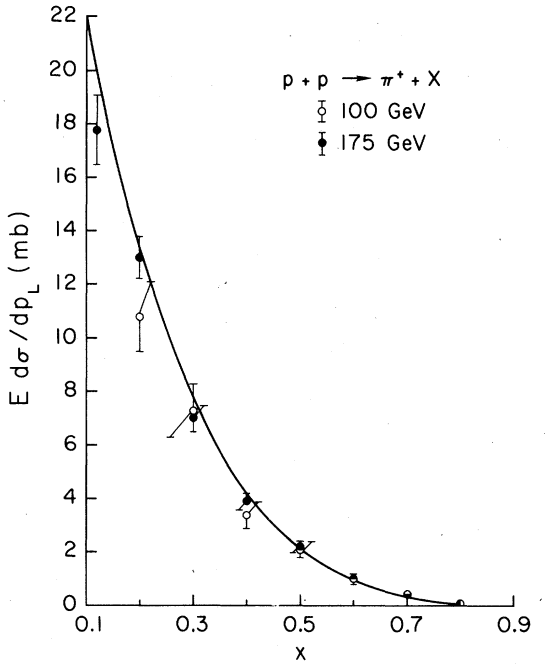

FIG. 10. Theoretical prediction (solid line) compared to the data (Ref. 31) for the inclusive cross section $pp \to \pi^+ X$ at 100 and 175 GeV.

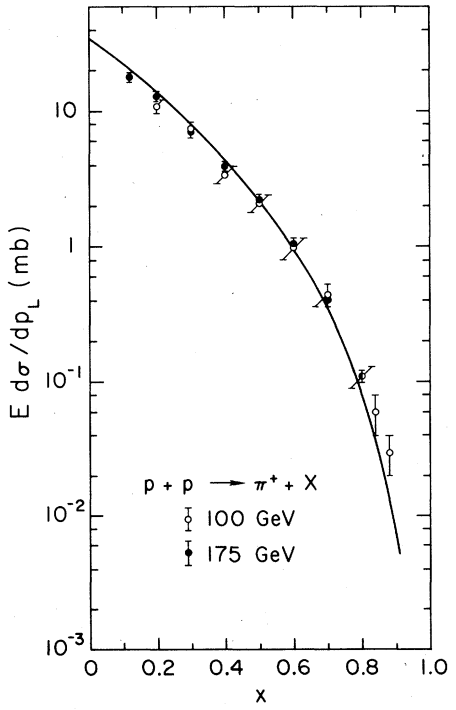

FIG. 9. Theoretical prediction (solid line) compared to the data (Ref. 31) for the inclusive cross section $pp \to \pi^+ X$ at 100 and 175 GeV.

of the nucleon structure function is done. Then the π^+/π^- ratio of the meson spectra can be calculated.

We have emphasized in this paper the formulation of the low-p_T problem. Application of the formalism to various specific reactions can be carried out without basic complication. For the production of strange mesons and baryons, for example, the effects of quark masses as well as three-valon recombinations can be investigated on the basis of the analysis described in Secs. II and III. Particle correlation can also be studied. A better determination of the evolution parameter ζ can be made if we replace νW_2 by the inclusive cross section of $pp \to \pi^+ X$ as a phenomenological input. At the sacrifice of not predicting that one reaction, we gain a reliable value of ζ for low-p_T reactions, which can then be used to calculate the cross sections for all other reactions, including those initiated by meson beams. The idea here is that the evolution from valons to partons should be the same in all low-p_T reactions, whether they are in mesons, nucleons, or even hyperon beam particles. The parameter c in (5.23) for the sea distribution is most probably independent of the hadron, and the parameter $\tilde{a}$ can be determined as indicated in this paper. Since the valon distributions are already given in Sec. II, we therefore have at hand a tight scheme that allows one to calculate the inclusive cross sections of all hadronic reactions. Of course, we are optimistic that the agreement with data will be good.

ACKNOWLEDGMENT

I have benefitted from discussions with Dr. G. Brandenburg and Dr. E. Takasugi. This work was supported in part by the U. S. Department of Energy under Contract No. EY-76-S-06-2230.

APPENDIX

We want to evaluate

$$K_{\rm NS}(m,n) = \int_0^1 dz\, z^{m-2}(1-z)^{n-1} K_{\rm NS}(z) . \qquad \text{(A1)}$$

Since we know the moments $K_{\rm NS}(n)$, we have by Mellin transform

$$K_{\rm NS}(z) = \frac{1}{2\pi i} \int_{c-i\infty}^{c+i\infty} dl\, z^{-l+1} K_{\rm NS}(l) . \qquad \text{(A2)}$$

Substitution into (A1) yields

$$K_{\rm NS}(m,n) = \frac{1}{2\pi i} \int_{c-i\infty}^{c+i\infty} dl\, K_{\rm NS}(l) B(m-l,n) . \qquad \text{(A3)}$$

The integrand has simple poles at $l=m$, $m+1,\ldots,$ and $m+n-1$. Letting $k=l-m$, and using the identity

$$\Gamma(-k) = \pi/[\Gamma(k+1)\sin\pi(k+1)] , \qquad \text{(A4)}$$

we have for the residues at the poles of $B(-k,n)$

$$(-1)^{k+1}\Gamma(n)/[\Gamma(k+1)\Gamma(n-k)] .$$

It then follows from contour integration of (A3) that

$$K_{\rm NS}(m,n) = \sum_{k=0}^{n-1} \frac{(-1)^k}{n} [B(k+1,n-k)]^{-1} K_{\rm NS}(m+k) . \qquad \text{(A5)}$$

[1]For recent reviews see R. C. Hwa, in *Proceedings of IX International Symposium on High Energy Multiparticle Dynamics, Tâbor Czechoslovakia, 1978* (Czechoslovak Academy of Science, Institute of Physics, Prague, 1978); L. Van Hove, Schladming Lecture, 1979 (unpublished) [Report No. TH. 2628-CERN (unpublished)].

[2]W. Ochs, Nucl. Phys. B118, 397 (1977).

[3]K. P. Das and R. C. Hwa, Phys. Lett. 68B, 459 (1977).

[4]R. Blankenbecler and S. J. Brodsky, Phys. Rev. D 10, 2973 (1974).

[5]R. C. Hwa and R. G. Roberts, Z. Phys. C 1, 81 (1979).

[6]D. W. Duke and F. E. Taylor, Phys. Rev. D 17, 1788 (1978).

[7]J. Kuti and V. F. Weisskopf, Phys. Rev. D 4, 3418 (1971).

[8]T. A. DeGrand and H. I. Miettinen, Phys. Rev. Lett. 40, 612 (1978); T. A. DeGrand, Phys. Rev. D 19, 1398 (1979).

[9]E. Takasugi, Z. Tata, C. B. Chiu, and R. Kaul, Phys. Rev. D 20, 211 (1979); E. Takasugi and X. Tata, *ibid.* 21, 1838 (1980).

[10]T. A. DeGrand, D. W. Duke, T. Inami, H. I. Miettinen, J. Ranft, and H. Thacker (unpublished).

[11]V. Chang and R. C. Hwa, Phys. Lett. 85B, 285 (1979).

[12]V. Chang and R. C. Hwa, Phys. Rev. Lett. 44, 439 (1980).

[13]R. C. Hwa, Phys. Rev. D 22, 759 (1980).

[14]R. P. Feynman, Phys. Rev. Lett. 23, 1415 (1969).

[15]G. Altarelli and G. Parisi, Nucl. Phys. B126, 298 (1977).

[16]B. Andersson, G. Gustafson, and C. Peterson, Phys. Lett. 69B, 221 (1977); A. Capella, U. Sukhatme, C. I. Tan, and J. Trân Thanh Vân, Phys. Lett. 81B, 68 (1979); A. Capella, U. Sukhatme, and J. Trân Thanh Vân, Orsay Report No. LPTPE 79/23, 1979 (unpublished); G. Cohen-Tannoudji, A. El Hassouni, J. Kalinowski, O. Napoly, and R. Peschanski, Phys. Rev. D 21, 2699 (1980).

[17]S. J. Brodsky and J. F. Gunion, Phys. Rev. D 17, 848 (1978).

[18]J. F. Gunion, Phys. Lett. (to be published).

[19]G. Altarelli, N. Cabibbo, L. Maiani, and R. Petronzio, Nucl. Phys. B69, 531 (1974); N. Cabibbo and R. Pe-

tronzio, *ibid.* B137, 395 (1978).
[20]T. A. DeGrand, Nucl. Phys. B151, 485 (1979).
[21]P. C. Bosetti *et al.*, Nucl. Phys. B142, 1 (1978).
[22]J. G. H. de Groot *et al.*, Phys. Lett. 82B, 292 (1979); 82B, 456 (1979).
[23]A. Para (private communication); see also, in *Proceedings of the 1979 International Symposium on Lepton and Photon Interactions at High Energies, Fermilab*, edited by T. B. W. Kirk and H. D. I. Abarbanel (Fermilab, Batavia, Illinois, 1979).
[24]C. B. Newman *et al.*, Phys. Rev. Lett. 42, 951 (1979); J. E. Pilcher, in *Proceedings of the 1979 International Symposium on Lepton and Photon Interactions at High Energies, Fermilab*, edited by T. B. W. Kirk and H. D. I. Abarbanel (Fermilab, Batavia, Illinois, 1979).
[25]S. D. Drell and T. M. Yan, Phys. Rev. Lett. 25, 316 (1970).
[26]G. W. Brandenburg (private communication); a paper on the subject is in preparation.
[27]G. P. Lepage and S. J. Brodsky, Phys. Rev. Lett. 43, 545 (1979); 43, 1625 (E) (1979); A. Duncan and A. H. Mueller, Phys. Rev. D 21, 1636 (1980).
[28]R. D. Field and R. P. Feynman, Phys. Rev. D 15, 2590 (1977).
[29]G. Miller *et al.*, Phys. Rev. D 5, 528 (1972).
[30]E. L. Berger, in *New Results in High Energy Physics—1978*, proceedings of the Third International Conference at Vanderbilt University on High Energy Physics, edited by R. S. Panvini and S. E. Csorna (AIP, New York, 1978).
[31]G. W. Brandenburg and V. A. Polychronakos (private communication). I am grateful to them for permitting me to use the preliminary data of Fermilab Experiment No. E118 (unpublished).
[32]F. E. Taylor *et al.*, Phys. Rev. D 14, 1217 (1976).
[33]J. Singh *et al.*, Nucl. Phys. B140, 189 (1978).
[34]D. Cutts *et al.*, Phys. Rev. Lett. 43, 319 (1979).